Journal of Hazardous Materials 189 (2011) 134–140

Contents lists available at ScienceDirect

Journal of Hazardous Materials

journal homepage: www.elsevier.com/locate/jhazmat

A modeling and experimental study of flue gas desulfurization in a dense phase tower

Guanqin Chang*, Cunyi Song, Li Wang

School of Civil and Environmental Engineering, University of Science and Technology Beijing, Beijing 100083, PR China

ARTICLE INFO

Article history:
Received 3 December 2010
Received in revised form 28 January 2011
Accepted 4 February 2011
Available online 5 March 2011

Keywords:
Flue gas desulfurization
Dense phase tower
Ca/S molar ratio
Sulfur dioxide

ABSTRACT

We used a dense phase tower as the reactor in a novel semi-dry flue gas desulfurization process to achieve a high desulfurization efficiency of over 95% when the Ca/S molar ratio reaches 1.3. Pilot-scale experiments were conducted for choosing the parameters of the full-scale reactor. Results show that with an increase in the flue gas flow rate the rate of the pressure drop in the dense phase tower also increases, however, the rate of the temperature drop decreases in the non-load hot gas. We chose a water flow rate of 0.6 kg/min to minimize the approach to adiabatic saturation temperature difference and maximize the desulfurization efficiency. To study the flue gas characteristics under different processing parameters, we simulated the desulfurization process in the reactor. The simulated data matched very well with the experimental data. We also found that with an increase in the Ca/S molar ratio, the differences between the simulation and experimental data tend to decrease; conversely, an increase in the flue gas flow rate increases the difference; this may be associated with the surface reactions caused by collision, coalescence and fragmentation between the dispersed phases.

1. Introduction

Acid rain has acquired considerable concern in past decades because of the extent of its harm to the global environment. Sulfur dioxide (SO_2) waste released from fossil fuel combustion has been commonly accepted as the main cause of acid rain. Removal of SO_2 from the flue gas emitted during combustion of fossil fuels has been the focus of research worldwide since the 1970s. SO_2 poses a considerable threat to ecosystems, building materials, agriculture, as well as human health. In particular, SO_2 pollution is a very serious problem in large and mid-sized Chinese cities, where a cost efficient and highly effective desulfurization means is urgently needed [1]. Depending on the involvement of water during the desulfurization process, and how desulfurization products are dealt with, flue gas desulfurization (FGD) technology can be divided into wet, semi-dry, and dry processes [2]. Among these, the wet FGD process is the main technology used for flue gas desulfurization, which has the advantages of high desulfurization efficiency, high utilization rate of desulfurization reagents, and a stable operating environment [3–5]. Rajmohan et al. reported the removal of SO_2, as well as particulate pollutants, with an almost 99.99% efficiency [6–8]. Meikap et al. achieved 100% SO_2 removal efficiency when employing a modified multi-stage bubble column scrubber [9,10]. However, the main disadvantage of the wet scrubber is the fact that it is only suitable for flue gas desulfurization of large-scale coal-fired power plants. Moreover, the wet process has many other disadvantages, such as, the complexity of the system, which occupies a large area, high-energy consumption, severe corrosion, and extensive wastewater treatment, in addition to the large initial investment that is required [5]. In contrast, the dry process requires no discharge, has minor equipment corrosion, and is a simple structure easily maintained, as well as having a low operating cost. However, the desulfurization efficiency and utilization rate of the desulfurization reagent for the dry process are very low, which dramatically limits the application of the dry process [2].

Compared to the wet and dry process, semi-dry FGD combines advantages of both dry and wet processes, for example, rapid reaction speed, high desulfurization efficiency, and no discharge [11,12]. However, there are problems associated with semi-dry FGD technology, such as low utilization rate of desulfurization, choking phenomenon and large consumption of desulfurizer and space. To meet the standards of SO_2 removal, great efforts have been made to develop new FGD technologies with less/no waste, low cost and high efficiency [13,14].

Spray-dryer and CFB-FGD processes are two traditional semi-dry processes. Spray-dryer process has been extensively tested. However, a great drawback of this method is its large space consumption in order to maintain long flue gas residence time (10–15 s) for desulfurization reaction and slurry droplet evaporation, as well as to meet the requirement for the complicated slurrying system [15]. Circulating fluidized bed is also widely used for flue gas desulfurization, however, the choking phenomenon

* Corresponding author. Tel.: +86 10 6233 3434; fax: +86 10 62333201.
E-mail address: guanqinchang@gmail.com (G. Chang).

0304-3894/$ – see front matter © 2011 Elsevier B.V. All rights reserved.
doi:10.1016/j.jhazmat.2011.02.009

widely occurs due to unsteady flow in the bed resulting from the fact that flue gas and desulfurization reagent enter into the reactor from the bottom of the reactor, which seriously affect the efficiency of desulfurization [14,16].

Many new semi-dry process technologies have been invented in an attempt to achieve high SO_2 desulfurization efficiency at a low cost and small space consumption [17]. This paper presents data on the incorporation of a new type of semi-dry desulfurization equipment, the dense phase tower (DPT). DPT is defined as a desulfurization tower where flue gas and desulfurization reagent enter into DPT from the top of the reactor, which can prevent the choking phenomenon, thus ensuring high concentration of sorbent suspension. Moreover, flue gas superficial detention time was 5–12 s in the DPT, which dramatically reduce the size comparing to spray-dryer process. Therefore, the DPT takes the advantage of application on space-limited plants.

Flue gas first entered the DPT from a side entrance located at the top of the tower, then is mixed with the fresh desulfurization reagent and desulfurization circulating ash from a bucket elevator. The desulfurization ash is humidified as it passed through the humidifier. Finally, desulfurization ash and flue gas are distributed through a diversion plate, which is located right below the mechanical rakings. Flue gas flows downward along the tower and reacts with active ingredients of desulfurization in an effective reaction zone. After desulfurization, the flue gas enters a bag-type dust collector for dust removal and then purified flue gas is discharged from the flue channel. Meanwhile, circulating ash is transferred back to the reactor through the bucket elevator.

We used computational fluid dynamics (CFD) to simulate the temperature and pressure drop, desulfurization efficiency, temperature and pressure distribution, circulating ash concentration distribution and circulating ash trajectory. CFD provides a method to build and run models that can simulate gas dispersion in such geometrically complex situations. Based on a CFD analysis, the FLUENT software solves the three-dimensional Reynolds averaged equations for flow, pressure, turbulence parameters and concentration distribution.

Pilot-scale experiments on actual flue gas from Shijiazhuang Iron and Steel Co., Ltd., were performed using the DPT process. We studied the Ca/S molar ratio influence on desulfurization efficiency, water addition and the influence of flue gas flow rate on decreases in flue gas temperature and pressure. Pilot-data showed a good match with the theoretical simulation data. The experimental data provide the basis for the industrial scale operation of the factory. The simulated and experimental results have provided guidelines for the industrial applications of the DPT process in several power and sintering plants in China.

2. Materials and methods

2.1. Apparatus and procedure

The apparatus for the pilot DPT series of experiments is described as follows (Fig. 1). The reactor ($1.2 \times 1.2 \times 5.0$ m) included a vertical rectangular tower containing humidification, dust removal, and cycle-ash transport system. Six parallel mechanical rakings, totally contained within three internal layers, were installed at a position 3/4 of the way from the top of the DPT. The mechanical rakings, as well as the diversion plate located right below them, were made from manganese alloy steel. The humidification system consisted of a SJ5 bi-axial humidifier, water tanks, metering pumps, and other devices. Five to ten hollow water sprayers with a droplet size less than 40 μm were installed vertically on the four sides of the humidifier. The dust removal system included 88 low pressure $\Phi 130 \times 2000$ mm pulse-jet bags, a W-0.3/8-Pa air compressor, a 0.2 m^3 gas tank, submerged-type pulse

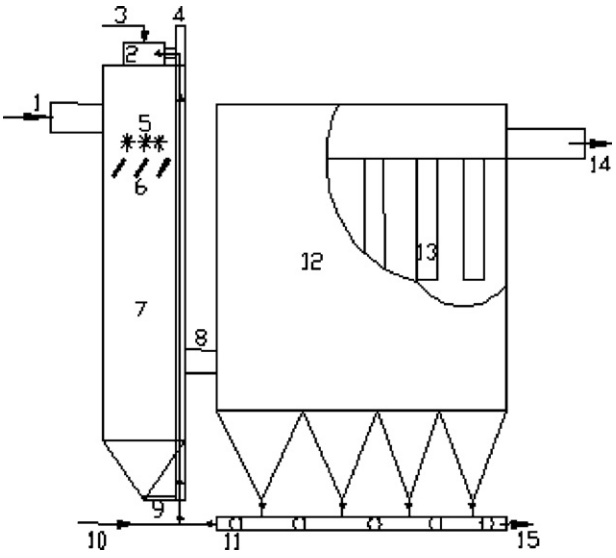

Fig. 1. Schematic diagram of the experimental setup: (1) Flue gas Inlet; (2) Humidification Unit; (3) Humidification Water; (4) Bucket Elevator; (5) Internal Mechanical Raking; (6) Internal Diversion Plate; (7) DPT Desulfurization Reactor; (8) Middle Flue gas Channel; (9) Tower Bottom Conveyor Scraper; (10) New Desulfurization reagent; (11) Circulating Ash Transport System; (12) Bag-type Dust Collector; (13) Bag; (14) Flue gas Outlet; (15) Discharge Ash.

valve and an integrated pulse meter control box. The cycle-ash transport system included a scraper conveyor in the lower part of the tower, a bag-type dust collector, a DL160-30 m bucket elevator and other devices for the removal of the desulfurization by-product. There were openings for testing and sampling flow, pressure, temperature, humidity, SO_2 concentration, dust concentration and other national standard parameters located on the tower body and outlet and inlet of the flue gas channel. Insulation materials (thickness: 50 mm) covered the outside of the tower. In addition, electric heating devices were installed on the top of the tower and part of the ash bucket. A schematic diagram of the test equipment is shown in Fig. 1.

2.2. Experimental flue gas and desulfurization reagent

The experimental device was built beside the flue gas channel of the #3 Sintering Machine Fan, which was located behind the electrostatic precipitator that is the pre-treatment unit for the sintering flue gas (in the Shijiazhuang Iron and Steel Co.). Test flue gas was produced by a high temperature sintering process. The SO_2 concentrate at the reactor entrance was the flue gas that came out of the electrostatic precipitator located right after the sintering plant; the SO_2 concentrate at the outlet of the reactor was the clean gas that came out of the bag-type dust collector. The desulfurization reagent was a white lime powder with mesh size ~100 and contained active ingredients totaling 89%. Flue gas flow rate was 2000–5000 Nm^3/h, temperature at the system inlet was 100–140 °C, flue gas superficial detention time was 5–12 s, SO_2 concentration in the flue gas inlet was 800–2000 mg/Nm^3, Ca/S molar ratio was 1.0–1.8, water flow rate was 0–0.75 kg/min. The mass flow rate of the reagent (lime) was 1.0–9.0 ton/h, and the recycle mass flow rate of ash was 5.0–50 kg/h.

3. Mathematical model

We used FLUENT to simulate the gas–solid flow in the DPT. FLUENT is a software program used for the simulation and analysis of fluid flow, chemical reaction and heat transfer in a complex geometry zone, after setting the boundary conditions.

3.1. Models and assumptions

3.1.1. Chemical reaction model

The chemical reaction that occurs between the active ingredient in desulfurization ash and SO_2 among flue gas is surface reaction.

The following assumptions were made: (1) Desulfurization ash particles are spherical particles and with the same size; (2) The only chemical reaction is between SO_2 and desulfurization ash particles; (3) The reaction is a first order reaction, instantaneous, and only in the gas–solid phase;

The reaction model is set as following:

$$\overline{R}_{j,\mathrm{r}} = A_\mathrm{p} h_\mathrm{r} Y_j p_\mathrm{n} \frac{R_{\mathrm{kin,r}} D_{0,\mathrm{r}}}{R_{\mathrm{kin,r}} + D_{0,\mathrm{r}}} \tag{1}$$

where $\bar{R}_{j,\mathrm{r}}$ (kg/s) is the consumption rate of the desulfurization ash particle surface material; A_p (m^2) is surface area of desulfurization ash particles; Y_j (j) is particle mass fraction of mass; η_r is efficiency factor; $R_{j,\mathrm{r}}$ ($\mathrm{kg/m^2\,s}$) is reaction rate of surface particle mass in per area unit; p_n (Pa) is partial pressure of gas phase substances; $D_{0,\mathrm{r}}$ is diffusion rate coefficient of reaction r; $R_{\mathrm{kin,r}}$ is the kinetic rate of reaction r; and N_r is explicit series of reaction r.

3.1.2. Gas turbulent flow model

Standard two-equation $k-\varepsilon$ model was used for flue gas turbulent flow. The following assumptions were made: (1) Gas turbulence is a fully turbulence; (2) The impact of molecular viscosity is omitted.

The $k-\varepsilon$ model is:

$$\rho\frac{Dk}{Dt} = \frac{\partial}{\partial x_i}[(\mu + \frac{\mu_1}{\sigma_k})\frac{\partial k}{\partial x_i}] + G_k + G_\mathrm{b} - \rho\varepsilon - Y_\mathrm{M} \tag{2}$$

$$\rho\frac{D\varepsilon}{Dt} = \frac{\partial}{\partial x_i}[(\mu + \frac{\mu_1}{\sigma_k})\frac{\partial \varepsilon}{\partial x_i}] + C_{1\varepsilon}\frac{\varepsilon}{k}(G_k + C_{3\varepsilon}G_\mathrm{b}) - C_{2\varepsilon}\rho\frac{\varepsilon^2}{k} \tag{3}$$

$$\mu_\mathrm{t} = \rho C_\mu \frac{k^2}{\varepsilon} \tag{4}$$

where μ_t is turbulence coefficient; G_b is turbulent kinetic energy due to buoyancy effects; G_k is turbulent kinetic energy due to average velocity gradient; Y_M is influence of expansion of the compressible turbulent fluctuation to the total dissipation rate; $C_{1\varepsilon}$, $C_{2\varepsilon}$ and C_μ are empirical constant; σ_k is Prandtl number corresponding with turbulent kinetic energy k; σ_ε is Prandtl number corresponding with dissipation rate ε.

3.1.3. Particle turbulence dissipation model

"Discrete Random Walk" model was used to determine desulfurization ash turbulence dissipation. The following assumptions were made: (1) Fluid fluctuating velocity is piecewise constant functions of time; (2) Omitting the impact of molecular viscosity.

The Discrete Random Walk model is:

$$t_\mathrm{cross} = -\tau\ln(1 - \frac{L_\mathrm{e}}{\tau\left|u - u_\mathrm{p}\right|}) \tag{5}$$

where t_cross (s) is the time of particle through the turbulent eddy; τ (s) is the particle relaxation time; L_e (m) is eddy length scale; $\left|u - u_\mathrm{p}\right|$ (m/s) is velocity difference between particles and fluid.

3.1.4. Particle motion equation

The Lagrangian approach was used to determine gas and particle flow field by tracking the trajectories of particles and gas. In the DPT, the temperature difference between inlet and outlet is about 50 °C, and the temperature gradient is relatively small, so thermophoresis force can be ignored. We also ignore the Brownian force and Saffman lift, since desulfurization ash particle size is generally greater than 10 μm. The force equation only considered gravity of desulfurization ash, gas drag force and rotating driving force caused by internal components inside the DPT.

The following assumptions were made: (1) Gas and solid phase occupied a different space; (2) Gas and solid phase are both continuous. Gas phase is Newtonian fluid, and the two phases are coexistence and mutual penetration with determined physical parameters; (3) Desulfurization ash particles are smooth rigid spheres with the same size, and only considering the collision between two spheres.

Motion equation of desulfurization ash in DPT reactor:

$$\frac{du_{x,\mathrm{p}}}{dt} = \frac{18\mu}{\rho_\mathrm{p} d_\mathrm{p}^2}\frac{C_\mathrm{D}Re}{24}(u_x - u_{x,\mathrm{p}}) + \frac{g_x(\rho_\mathrm{p} - \rho)}{\rho_\mathrm{p}} + (1 - \frac{\rho}{\rho_\mathrm{p}})\Omega^2 x + 2\Omega(u_{y,\mathrm{p}} - \frac{\rho}{\rho_\mathrm{p}}u_y) \tag{6}$$

where ρ ($\mathrm{kg/m^3}$) is flue gas density; ρ_p ($\mathrm{kg/m^3}$) is particle density; d_p (m) is particle diameter; C_D is drag coefficient; Re is desulfurization ash particle Reynolds number; Ω (rad/s) is angular velocity of circular motion of desulfurization ash particles.

3.1.5. Heat transfer model

To simulate the complicated heat transfer process in DPT, the following assumptions were made:

(1) Not consider the chemical reaction and ignore thermal radiation; (2) Assume desulfurization ash particle is spherical shape and ignore the interaction between desulfurization ash particles; (3) The internal temperature of desulfurization ash particle is uniform distribution, that is, the internal temperature gradient is ignored and heat transfer only occurs between gas and solid phase.

When desulfurization ash particles temperature is lower than its evaporation temperature, and no more water inside the particle, the following laws are employed:

$$T_\mathrm{p} < T_\mathrm{vap} \tag{7}$$

$$m_\mathrm{p} \le (1 - f_{\mathrm{v},0})m_{\mathrm{p},0} \tag{8}$$

$$m_\mathrm{p}c_\mathrm{p}\frac{dT_\mathrm{p}}{dt} = A_\mathrm{p}\left\{-[h + \varepsilon_\mathrm{p}\sigma T_\mathrm{p}^3]T_\mathrm{p} + [hT_\infty + \varepsilon_\mathrm{p}\sigma\theta_\mathrm{R}^4]\right\} \tag{9}$$

where T_p (K) is particle temperature; T_vap (K) is particle evaporation temperature; $f_{\mathrm{v},0}$ is water ratio in the particle; $m_{\mathrm{p},0}$ (kg) is particle initial mass; m_p (kg) is particle mass; c_p (J/kg K) is specific heat of the particle; A_p (m^2) is the surface area of the particle; T_∞ (K) is the flue gas temperature; h ($\mathrm{W/m^2\,K}$) is convective heat-transfer coefficient; ε_p is radiance; σ ($\mathrm{W/m^2\,K^4}$) is a Stephen Sun Boltzmann constant; θ_R (K) is radiation temperature; d_p (m) is the diameter of desulfurization ash particle; k_∞ is thermal conductivity of flue gas.

3.2. Boundary condition of DPT modeling

3.2.1. Turbulence quantity

In most turbulent flows, higher-level turbulence is derived from the boundary layer rather than the zone where boundary flows enter the basin, which results in a flow that is relatively insensitive to the boundary value. When turbulence intensity is ≤1%, it is called low intensity turbulence; conversely, turbulence intensity >10%, is called high intensity turbulence. Measurement data from outside the entrance of the border can accurately estimate turbulence intensity. For internal flow, turbulence intensity at the entrance depends entirely on the upstream flow. If the upstream flow has not developed fully or has not been disturbed, we instead use low turbulence intensity. If the upstream flow has developed fully, turbulence intensity may reach several percent.

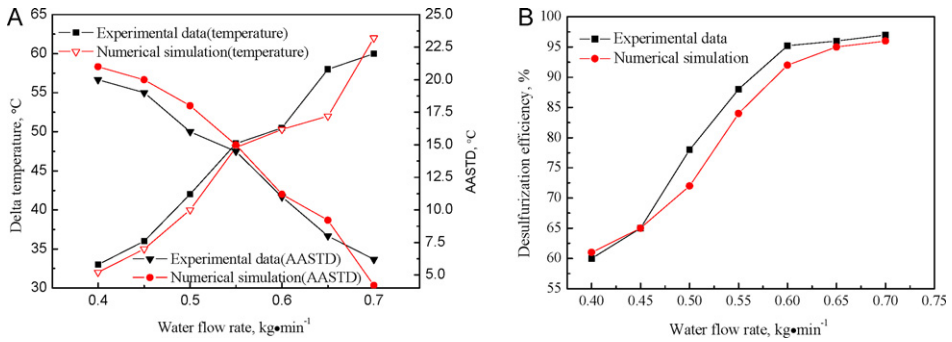

Fig. 2. Effect of water flow rate on flue gas temperature drop, ASSTD and desulfurization efficiency in DPT.

3.2.2. Boundary condition for velocity entrance

The velocity boundary condition was used to define the flow velocity and properties and other related scalar quantities. This boundary condition is applicable to incompressible flow but not to compressible flow, since compressible flow allows fluctuation stagnation conditions that result in large errors.

3.2.3. Boundary condition for pressure exit

The exit of the DPT connects with the entrance of the bag-type dust collector. The conditions for the exit boundary pressure require a specified static pressure at the exit boundary. The relative experimental static pressure was within −800 to −900 Pa at the connection spot. In this paper, the value of static pressure in the simulation was set to −850 Pa.

3.2.4. Boundary conditions for the wall

The wall boundary is used to limit fluid and solid regions. In a viscous flow, the wall is the default non-slip boundary condition. The DPT body is a typical thermal boundary. In the numerical simulation, we assumed that the wall was made of 5 mm thick carbon steel. The value of the thermal boundary is 1000 W/m^2 in the winter, 600 W/m^2 in the summer and 800 W/m^2 in the spring and fall.

4. Results and discussion

4.1. Influence of water flow rate on flue gas temperature

Water spray is an important way to achieve high desulfurization efficiency through activation of the desulfurization reagent in the DPT. Yet, water spray can also reduce flue gas temperature and cause corrosion in the DPT and bag-type dust collector. In addition, an increasing in the moisture content will increase the chances of scaling. Choosing a suitable water flow rate is an important way to guarantee the normal operation of the DPT. Fig. 2(A) shows the relationship between water flow rate and the drop in flue gas temperature drop (Delta temperature) in the DPT. The graph also shows the relationship between water flow rate and the approach to an adiabatic saturation temperature difference (AASTD), such that delta temperature increases in the DPT were associated with an increase in water flow rate. Fig. 2(B) shows the relationship between water flow rate and desulfurization efficiency, such that an increase in water flow rate was also associated with an increase in desulfurization efficiency.

In an appropriate engineering design, AASTD should be >10 °C in order to prevent corrosion and scaling. When water flow rates were 0.6 kg/min and 0.7 kg/min, the CSATD were 11 °C and 6.2 °C, and desulfurization efficiency reached 95.2% and 97% respectively. Despite that the improvement in desulfurization efficiency was not so obvious, the decrease in AASTD was significant. When water addition was 0.6 kg/min, the AASTD was at its lowest value under safe operating conditions. On this basis, we chose a water flow rate value of 0.6 kg/min.

4.2. Influence of flue gas flow rate on pressure and temperature

Pressure and temperature were measured when flue gas volumes were 2000 Nm^3/h to 5000 Nm^3/h.

Fig. 3 shows the relationship between flue gas flow rate vs. delta pressure and delta temperature in the DPT, such that, there is a decrease in the DPT negative pressure as the flue gas flow rate increases. The delta pressure was around 600 Pa when the flue gas flow rate was 3000 Nm^3/h, and the delta pressure increased to 1500 Pa when flow rate reached 5000 Nm^3/h. In the graph, the simulation values are slightly less than experimental ones, because the geometry of the model was completely idealized in the simulation. In this model, we assumed that the inside surface of the DPT was uniformly rough. In fact, existing geometric deviations increased the pressure drop in the DPT. The pressure changes in the numerical simulation and pilot-scale tests were 576 and 590 Pa, respectively, when the flow rate was 3000 Nm^3/h.

The temperature changes shown in Fig. 3 are non-loaded (i.e. no water and desulfurization reagent were added) in the hot gas, in which the change in the flue gas temperature decreases with an increase in flow rate. When the flow rate was reduced to 2000 Nm^3/h, the delta temperature of flue gas was about 7.3 °C, whereas, when the flow rate increased up to 5000 Nm^3/h, the delta temperature of flue gas was about 5.8 °C. For the same reason as stated previously, the simulation values were less than the experimental values. Moreover, negative pressure inside the tower leads to an additional temperature drop, as leakages are inevitable. The difference was more apparent when the outside temperature was lower in the winter. When the flow rate was 3000 Nm^3/h, the delta temperature in the numerical simulation and the pilot-scale test were 6.55 °C and 6.75 °C, respectively.

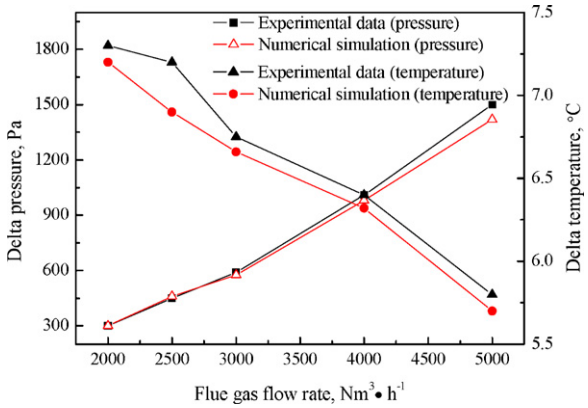

Fig. 3. Effect of flue gas flow rate on pressure and temperature in the DPT.

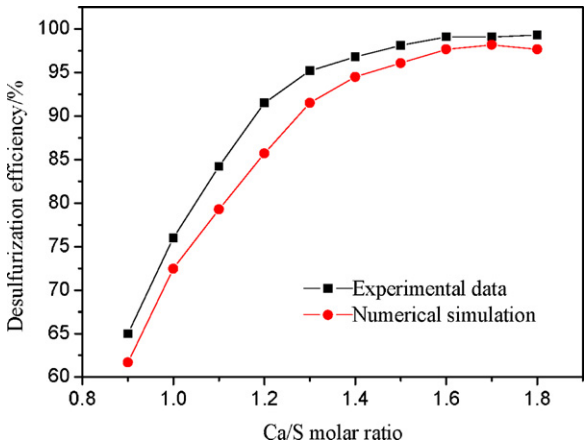

Fig. 4. Effect of Ca/S molar ratio on desulfurization efficiency.

4.3. Ca/S molar ratio influence on desulfurization efficiency

The Ca/S molar ratio is one of the most important control factors in the dense tower desulfurization process and it directly affects the chemical reaction between the desulfurization reagent and SO_2. The KM900 tester (KANE Company, England) was used to test SO_2 concentration at the flue gas inlet and outlet. Results showed that SO_2 concentration at flue gas entrance was 1200 mg/Nm^3 when flue gas flow-rate was 3000 Nm^3/h.

The graph of Ca/S molar ratio vs. desulfurization (Fig. 4) shows that values of the desulfurization efficiency in the pilot-scale experiment and the simulation increase as the Ca/S molar ratio increases. Moreover, when the Ca/S molar ratio reached 1.0–1.3, the desulfurization efficiency increased rapidly, and reached a plateau of over 95% at Ca/S molar ratios above 1.3. Therefore, we chose 1.3 as Ca/S molar ratio in the full-scale FGD process to achieve relatively high desulfurization efficiency.

The desulfurization efficiency value from the numerical simulation was always less than 3.9% lower than the value in the pilot-scale test. The main reason for this result is that in the numerical calculation we only considered the surface reactions of the desulfurization reagent, and neglected the new surface reactions resulting from collision, coalescence and fragmentation between the dispersed phases. New surface reactions become weaker with an increase in the Ca/S molar ratio, so that the differences between the simulation and experimental data tend to decrease in this situation. Another possible reason was air leakage and dilution of flue gas concentration. However, in those cases where a high desulfurization ratio is required (e.g. desulfurization efficiency >95%, reported by Rajmohan et al. [6–8] and Meikap et al. [9,10]), a wet scrubber can be applied.

Fig. 5 indicates the SO_2 concentration (A) and distribution of $Ca(OH)_2$ mass (B) when the Ca/S molar ratio was 1.0. The figures show that SO_2 reacts rapidly with $Ca(OH)_2$ in the circulating ash that enters the tower from the top of the equipment. The change in SO_2 concentration corresponds to the change in the gradient of the $Ca(OH)_2$ mass fraction. SO_2 concentration was reduced by around 30%, and the $Ca(OH)_2$ mass fraction was almost zero at the tower exit, which indicates that it is hard to ensure high desulfurization efficiency, but easy to achieve a high $Ca(OH)_2$ utilization rate with a lower Ca/S molar ratio.

4.4. Numerical simulation diagram

The numerical model was used to simulate the temperature and pressure distribution, trajectory of circulating ash and circulating ash concentration distribution inside the tower after the model was validated because it is difficult to obtain the data experimentally.

4.4.1. Temperature distribution in DPT

Fig. 6 shows a cross-section of the temperature distribution when using a water flow rate of 0.6 kg/min. The figure indicates that the temperature at tower entrance and exit were 398.7 K and 348.9 K, respectively. A higher temperature gradient forms in the area where hot flue gas makes contact with the desulfurization circulating ash, in which water evaporates rapidly, resulting in a rapid drop in flue gas temperature, and a dramatic flue gas adiabatic saturation temperature increase. Small differences between the flue gas temperature and flue gas adiabatic saturation temperature makes it easy to form a water film on the circulating ash surface, which is good for flue gas desulfurization. There was a zone near the top of the tower wall where the flue gas temperature was lower than the adiabatic saturation temperature, which resulted in circulating ash easily sticking onto the wall. During equipment maintenance in the pilot-scale test, this scaling and sticky phenomenon was obvious at the top of the tower wall. The tower-body temperature drop in the numerical simulation and the test were 50 °C and

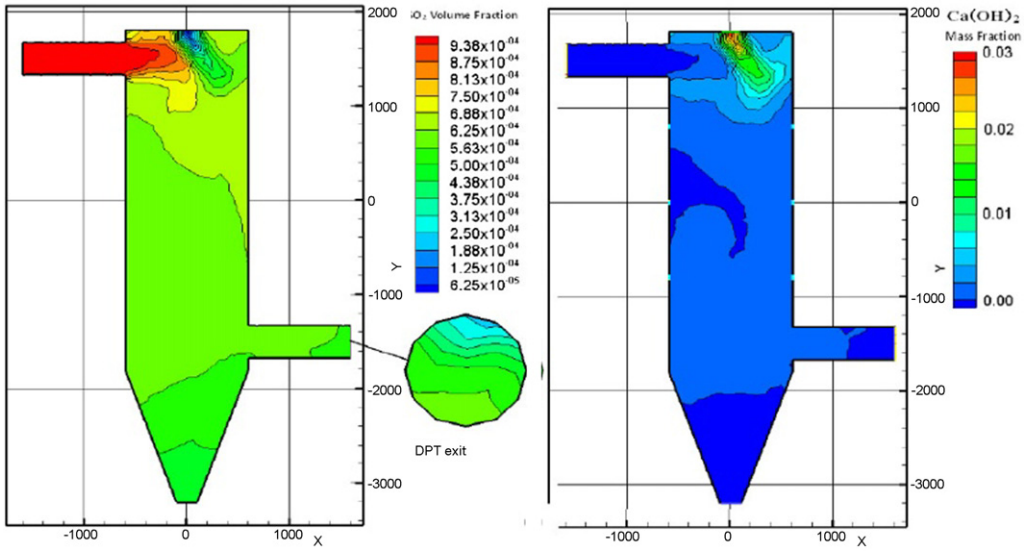

Fig. 5. Schematic cross-section of the tower exit showing the distribution of (A) SO_2 and (B) $Ca(OH)_2$ mass.

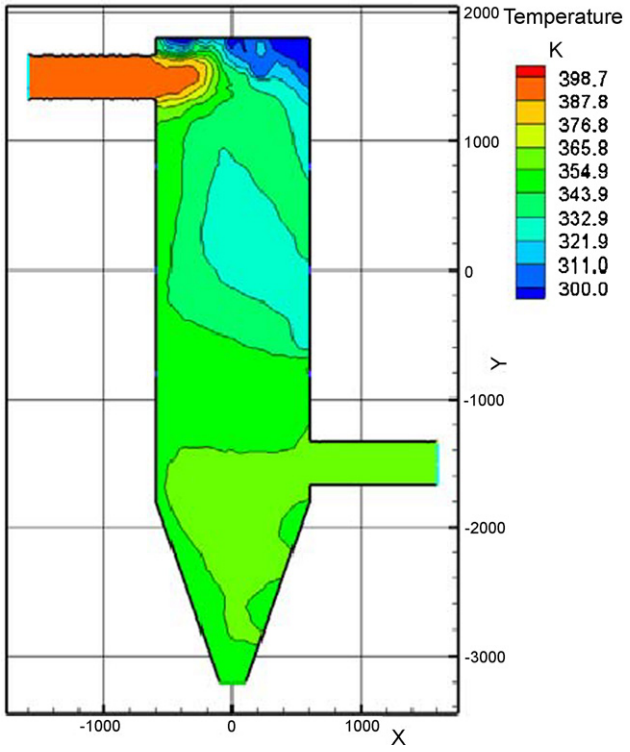

Fig. 6. Schematic cross-section showing the temperature distribution using a water flow rate of 0.6 kg/min.

49.8 °C, respectively, when the design flow rate was 3000 Nm^3/h and humidification capacity was 0.6 kg/min.

4.4.2. Pressure distribution

Similar to that found in other reactors, the DPT desulfurization system also has a pressure drop. Fig. 7 shows the pressure distribution when the flow rate was 2000 Nm^3/h, and indicates that the

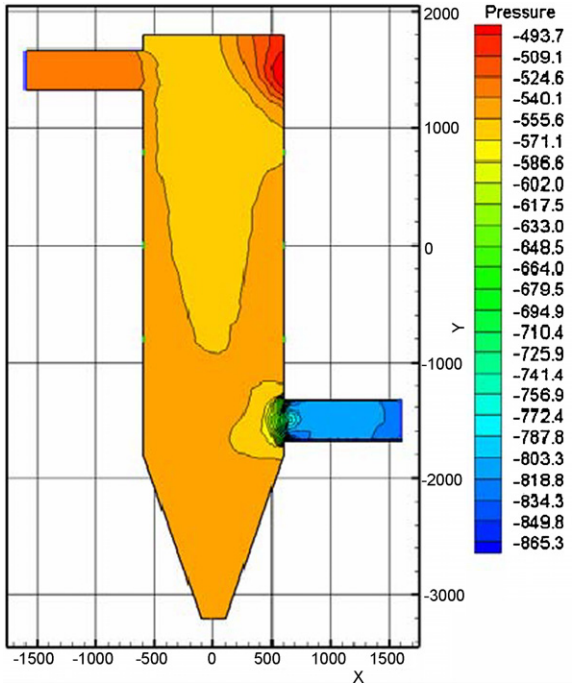

Fig. 7. Schematic cross-section showing the pressure distribution for a flow rate of 2000 Nm^3/h.

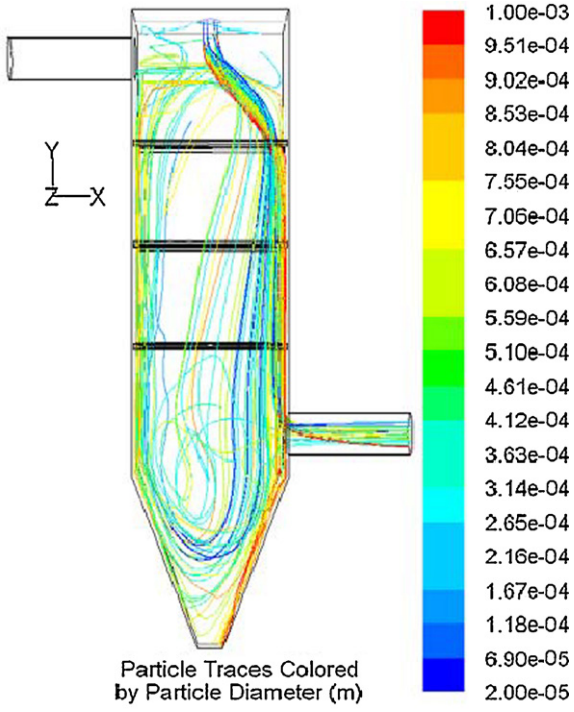

Fig. 8. Schematic cross-section showing the trajectory of circulating ash in the DPT.

pressure drop was 80 Pa at the inlet and effective reaction zone and was 300 Pa at the outlet. Therefore, the design optimization of tower outlet is a key process in reducing the pressure drop.

4.4.3. Circulating ash trajectory

The drag force from flue gas drives circulating ash movement, which directly affects the circulating ash mass distribution in the ash bucket and bag-type dust collector. In addition, the number, shape and location etc. of all internal elements have a significant influence on the circulating ash trajectory, and all these factors can affect its trajectory. Higher desulfurization efficiencies can be achieved when the distribution of circulating ash becomes more uniform. In engineering terms, the less circulating ash that goes into the bag-type dust collector, the less power is consumed for transporting and enhancing the circulating ash.

Fig. 8 shows the trajectory of the circulating ash when the flue gas flow rate was 3000 Nm^3/h. A C eddy formed by the flow of flue gas apparently drives circulating ash, and the majority of the ash forms a closed loop cycle in the tower. Most of the circulating ash with a size greater than 600 μm was deposited directly into the ash bucket, however, almost all the circulating ash <300 μm was carried to bag-type dust collector by the flue gas.

In the numerical simulation, we did not consider collision, coalescence and fragmentation between the dispersed phases. In a full-scale reactor, larger flue gas flow rates applies greater drag force on the circulating ash that results in more chances for collision, coalescence and fragmentation between circulating ash. Therefore, greater flue gas flow rates leads to larger differences between the simulation and experimental data.

5. Conclusions

We reported on a novel semi-dry FGD process to be employed for SO_2 removal. The influence of water flow rate on the drop in flue gas temperature was analyzed in order to optimize the desulfurization efficiency. The ASSTD were 11 °C and 6.2 °C with water flow rates of 0.6 and 0.7 kg/min respectively. We chose a water flow rate value of

0.6 kg/min, since at this point AASTD is >10 and the desulfurization efficiency was 95.2%.

Desulfurization efficiency increased with an increase in the Ca/S molar ratio, reaching over 95% when Ca/S molar ratio was 1.3. Therefore, we chose 1.3 as the Ca/S molar ratio for use in the full-scale FGD process in order to achieve relatively high desulfurization efficiency and low amounts of spent desulfurization reagent.

As flue gas flow rate increases, there is an increasing pressure drop in the DPT and a decreased temperature drop. The simulation values are slightly less than experimental ones, because of the completely idealized geometry of the model in the simulation. In fact, existing geometric deviations increased the pressure drop in the DPT. flow rate was 3000 Nm^3/h. Moreover, negative pressure inside the tower leads to temperature drop, as leakages are inevitable.

We also simulated desulfurization efficiency, and found that the difference between the simulation and pilot-scale experiment was less than 3.9%. Pilot-scale data matched very well with the theoretical simulation. The mathematical model and experimental results have been applied as guidelines for the industrial application of the DPT process in several power and sintering plant environmental processing projects, for example, Shijiazhuang Iron and Steel Co., Ltd. and Panzhihua Power Plant, which will be reported elsewhere.

Acknowledgments

The authors thank Dr. Thomas FitzGibbon for comments on previous drafts of the manuscript. This work was supported by the Shijiazhuang Iron and Steel Co., Ltd. (No. 32100183).

References

[1] Y. Zhao, S. Wang, L. Duan, Y. Lei, P. Cao, J. Hao, Primary air pollutant emissions of coal-fired power plants in China: current status and future prediction, Atmospheric Environment 42 (2008) 8442–8452.
[2] M. Miller, Retrofit SO_2 and NO_x control technologies for coal-fired power plants, Environmental Progress 5 (1986) 171–177.
[3] C.Y. Chu, S.J. Hwang, Flue gas desulfurization in an internally circulating fluidized bed reactor, Powder Technology 154 (2005) 14–23.
[4] C.F. Liu, S.M. Shih, Effect of NaOH addition on the reactivities of iron blast furnace slag/hydrated lime sorbents for low-temperature flue gas desulfurization, Industrial and Engineering Chemistry Research 43 (2004) 184–189.
[5] F. Scala, M. D'Ascenzo, A. Lancia, Modeling flue gas desulfurization by spray-dry absorption, Separation and Purification Technology 34 (2004) 143–153.
[6] B. Rajmohan, S. Biswas, B.C. Meikap, Performance characteristics of the particulates scrubbing in a counter-current spray-column, Separation and Purification Technology 61 (2008) 96–102.
[7] B. Rajmohan, R.K. Jain, B.C. Meikap, Comprehensive analysis for prediction of dust removal efficiency using twin-fluid atomization in a spray scrubber, Separation and Purification Technology 63 (2008) 269–277.
[8] B. Rajmohan, S.N. Reddy, B.C. Meikap, Removal of SO_2 from industrial effluents by a novel twin fluid air-assist atomized spray scrubber, Industrial and Engineering Chemistry Research 47 (2008) 7833–7840.
[9] B.C. Meikap, G. Kundu, M.N. Biswas, A novel modified multi-stage bubble column scrubber for SO_2 removal from industrial off gases, Separation Science and Technology 37 (2002) 3421–3442.
[10] B.C. Meikap, G. Kundu, M.N. Biswas, Scrubbing of fly-ash laden SO_2 in modified multistage bubble column scrubber, AIChE Journal 48 (2002) 2074–2083.
[11] J. Zhang, C. You, S. Zhao, C. Chen, H. Qi, Characteristics and reactivity of rapidly hydrated sorbent for semidry flue gas desulfurization, Environmental Science and Technology 42 (2008) 1705–1710.
[12] Y. Zhou, X. Zhu, J. Peng, Y. Liu, D. Zhang, M. Zhang, The effect of hydrogen peroxide solution on SO_2 removal in the semidry flue gas desulfurization process, Journal of Hazardous Materials 170 (2009) 436–442.
[13] I. Dahlan, K.T. Lee, A.H. Kamaruddin, A.R. Mohamed, Evaluation of various additives on the preparation of rice husk ash (RHA)/CaO-based sorbent for flue gas desulfurization (FGD) at low temperature, Journal of Hazardous Materials 161 (2009) 570–574.
[14] B. Du, L.S. Fan, Characteristics of choking behavior in circulating fluidized beds for Group B particles, Industrial and Engineering Chemistry Research 43 (2004) 5507–5520.
[15] Y. Zhou, M. Zhang, D. Wang, L. Wang, Study on a novel semidry flue gas desulfurization with multifluid alkaline spray generator, Industrial and Engineering Chemistry Research 44 (2005) 8830–8836.
[16] B. Du, W. Warsito, L.S. Fan, ECT studies of the choking phenomenon in a gas–solid circulating fluidized bed, AIChE Journal 50 (2004) 1386–1406.
[17] J. Neathery, Model for flue-gas desulfurization in a circulating dry scrubber, AIChE Journal 42 (1996) 259–268.